Journal of Alloys and Compounds 509S (2011) S823–S826

Contents lists available at ScienceDirect

Journal of Alloys and Compounds

journal homepage: www.elsevier.com/locate/jallcom

Elaboration and characterization of unreported $(Pr,Nd)_5Ni_{19}$ hydrides

Lucille Lemort[a], Michel Latroche[a,*], Bernard Knosp[b], Patrick Bernard[b]

[a] ICMPE CMTR CNRS UMR 7182, 2-8 rue Henri Dunant, 94320 Thiais Cedex, France
[b] SAFT, Direction de la Recherche, 111-113 Boulevard Alfred Daney, 33074 Bordeaux, France

ARTICLE INFO

Article history:
Received 22 July 2010
Received in revised form 4 October 2010
Accepted 20 October 2010
Available online 3 November 2010

Keywords:
Pr_5Ni_{19}
Nd_5Ni_{19}
Intermetallics
Crystal structure
Metal hydrides

ABSTRACT

In this study two new compounds have been synthesized: Pr_5Ni_{19} and Nd_5Ni_{19}. The crystallographic structures as well as the thermodynamic properties of the hydrogen absorbing compounds Pr_5Ni_{19} and Nd_5Ni_{19} have been determined. Both compounds exist under two polymorphic types that can be described as the stacking along the *c* axis of two different subunits $[(Pr,Nd)_2Ni_4]$ and $[(Pr,Nd)Ni_5]$: the hexagonal (2*H*) Pr_5Co_{19}-type structure (space group $P6_3/mmc$) and the rhombohedral (3*R*) Ce_5Co_{19}-type structure (space group R-$3m$). The two compounds are able to form hydrides at room temperature, in the pressure range of 0–10 MPa. They show desorption pressure plateaux around 0.8 MPa for Pr_5Ni_{19} and 1 MPa for Nd_5Ni_{19} and exhibit capacities under 10 MPa of 1.33 wt% for Pr_5Ni_{19} and 1.17 wt% for Nd_5Ni_{19} at the first cycle.

1. Introduction

Since the discovery of the hydride-forming metals, many applications have been considered. Until now, the most popular of these applications is still hydrogen storage in NiMH batteries. However, to keep NiMH batteries competitive to other power sources, enhanced performances need to be obtained by developing new generation of compounds. In the last ten years, much attention was paid to the La–Mg–Ni system.

Studies have shown that $La_{1-y}Mg_yNi_x$ ($3 < x < 4$, $0 < y < 1$) type compounds exhibit specific capacities up to 410 mAh/g thanks to their structure and the substitution of the rare earth by magnesium [1], characterized by high hydrogen capacity, light weight and low cost.

In those compounds some of them can be described as the stacking along the *c* axis of two different subunits $[A_2B_4]$ and $[AB_5]$ where A is a rare earth or an alkali earth and B a transition metal. In the case of A_5B_{19} compounds, the structure can be described as a stacking $n[A_2B_4]/m[AB_5]$ with $n = 1$, $m = 3$ [2–5]. As $(La,Mg)_5Ni_{19}$ system was investigated [6–9], related systems $(Pr,Mg)_5Ni_{19}$ and $(Nd,Mg)_5Ni_{19}$ were also considered in order to obtained better lifetime. Prior to the ternary system, investigation is necessary for the binary systems Pr–Ni and Nd–Ni. Indeed the 2 phases Pr_5Ni_{19} and Nd_5Ni_{19} are not mentioned in the latest phase diagram [10,11].

In the present study, crystal structures and hydrogenation properties of the binary phases have been investigated.

2. Experimental

The compounds Pr_5Ni_{19} and Nd_5Ni_{19} were obtained by arc-melting of the pure components (3 N purity) under argon atmosphere. The ingots were melted 5 times to ensure good homogeneity and were annealed at 1100 °C for 35 days in a silica tube under vacuum before quenching to room temperature.

The obtained samples were then reduced into powder by mechanical pulverization down to 32 µm in particle size. Structural analysis was made at room temperature by X-ray powder diffraction using a Bruker D8 advance diffractometer with Cu Kα radiation, flat plate, Bragg Brentano geometry and back scattered rear graphite monochromator. Diffracted intensities were measured in the range 18° and 80° with a two-theta step of 0.04°. Experimental data were analysed by the Rietveld method using Fullprof program [12]. Chemical analysis was performed by electron probe micro-analysis (EPMA) using a CAMECA SX-100 to check the composition of the alloys. Chemical analysis was also performed by inductively coupled plasma optical emission spectrometry (ICP-OES) using a Vista-Pro-Axial.

Hydrogenation properties were measured by determination of the pressure–composition–temperature (PCT) curves using the Sievert's method for pressure between 0.1 and 10 MPa at room temperature. PCT curves were measured after 2 activation cycles for Pr_5Ni_{19} (absorption at 25 °C under 10 MPa and desorption under primary vacuum at 40 °C) and 3 cycles for Nd_5Ni_{19}.

3. Results

3.1. Crystallographic structure

The X-ray diffraction patterns of the Pr_5Ni_{19} and Nd_5Ni_{19} compounds are respectively shown in Fig. 1(a) and (b) and the microprobe analysis in Fig. 2(a) and (b). The samples are composed of three different phases. The first and the second ones are the two polymorphic types of the same phase: A_5Ni_{19}.

---

* Corresponding author. Tel.: +33 1 49 78 12 10; fax: +33 1 49 78 12 03.
E-mail addresses: michel.latroche@icmpe.cnrs.fr, latroche@glvt-cnrs.fr (M. Latroche).

0925-8388/$ – see front matter © 2010 Elsevier B.V. All rights reserved.
doi:10.1016/j.jallcom.2010.10.102

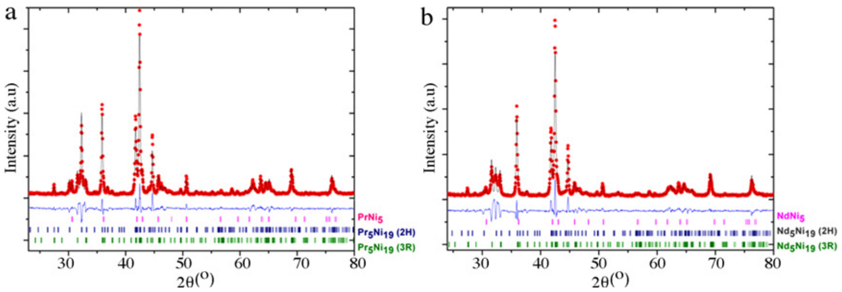

Fig. 1. Refined analysis of powder XRD data at room temperature for (a) Pr_5Ni_{19} and (b) Nd_5Ni_{19} (measured (dots), calculated (solid line) and difference curves (below); vertical bars correspond to line positions of the observed phases; radiation Cu Kα).

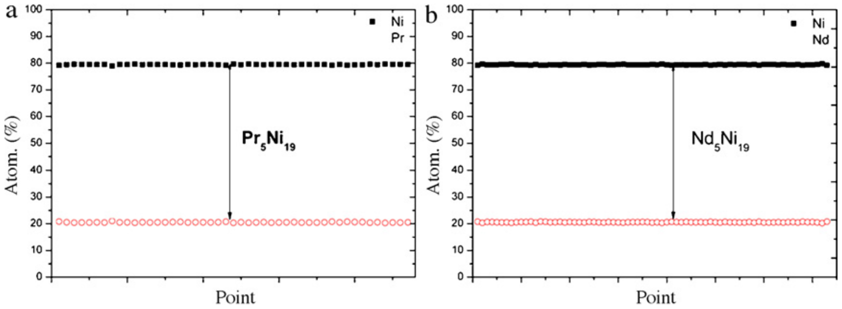

Fig. 2. Results from the microprobe analysis (EPMA) for (a) Pr_5Ni_{19} and (b) Nd_5Ni_{19} showing a constant composition of the sample despite the coexistence of the two polymorphic structures (2*H* and 3*R*).

The two polymorphic structures that coexist are the hexagonal (2*H*) Pr_5Co_{19}-type structure (space group *P*6₃/*mmc*) and the rhombohedral (3*R*) Ce_5Co_{19}-type structure (space group *R*-3*m*). The third minor phase is the hexagonal $CaCu_5$-type structure (space group *P*6/*mmm*). Phase amounts, lattice parameters and unit cell volume have been determined for the two samples by Rietveld refinement and are given in Tables 1 and 2.

The expected composition of Pr_5Ni_{19} and Nd_5Ni_{19} is $x = B/A = 19/5 = 3.8$. The EPMA allows to check the phase composition. Only one composition is observed for both compounds, $PrNi_{(3.88\pm0.08)}$ and $NdNi_{(3.86\pm0.07)}$ in agreement with the expected stoichiometry. $PrNi_5$ and $NdNi_5$ are not detected by EPMA, probably because of the low amount of these minor phases. No differences are found in composition of the two polymorphic phases. ICP

Table 1

Structural parameters for the binary compound Pr_5Ni_{19} showing coexistence of two isotypic forms of Pr_5Ni_{19}: 2*H* (space group *P*6₃/*mmc*) and 3*R* (space group *R*-3*m*). A third minor phase is detected: $PrNi_5$ with $CaCu_5$ type structure.

	Atoms	Sites	*x*	*y*	*z*	Occ.
Pr_5Ni_{19} Pr_5Co_{19}-type	Pr	$2c_1$	1/3	2/3	1/4	1
	Pr	$4f_1$	1/3	2/3	0.1325(7)	1
	Pr	$4f_2$	1/3	2/3	0.0222(8)	1
	Ni	$2a_1$	0	0	0	1
	Ni	$2b_1$	0	0	1/4	1
	Ni	$2d_1$	1/3	2/3	3/4	1
	Ni	$4e_1$	0	0	0.130(2)	1
	Ni	$4f_3$	1/3	2/3	0.872(2)	1
	Ni	$12k_1$	0.836(9)	2x	0.0653(8)	1
	Ni	$12k_2$	0.831(9)	2x	0.190(1)	1
Phase 2*H*-*P*6₃/*mmc*; 56 wt%; $a = 4.999(1)$ Å; $c = 32.410(7)$ Å; *V*/unit cell = 701.4(3) Å^3; $R_{bragg} = 6.5$; $R_p = 5.1$						
Pr_5Ni_{19} Ce_5Co_{19}-type	Pr	$3a_1$	0	0	0	1
	Pr	$6c_1$	0	0	0.079(1)	1
	Pr	$6c_2$	0	0	0.152(1)	1
	Ni	$3b_1$	0	0	1/2	1
	Ni	$6c_3$	0	0	1/4	1
	Ni	$6c_4$	0	0	1/3	1
	Ni	$6c_5$	0	0	0.416(4)	1
	Ni	$18h_1$	1/2	1/2	0.123(1)	1
	Ni	$18h_2$	1/2	1/2	0.042(2)	1
Phase 3*R*-*R*-3*m*; 37 wt%; $a = 4.998(1)$ Å; $c = 48.62(2)$ Å; *V*/unit cell = 1051.9(6) Å^3; $R_{bragg} = 7.5$; $R_p = 5.2$						
$PrNi_5$ $CaCu_5$-type	Pr	1*a*	0	0	0	1
	Ni	2*c*	1/3	2/3	0	1
	Ni	3*g*	1/2	0	1/2	1
Phase 2*H*-*P*6/*mmm*; 7 wt%; $a = 4.968(2)$ Å; $c = 3.968(2)$ Å; *V*/unit cell = 84.82(8) Å^3; $R_{bragg} = 6.3$; $R_p = 5.9$						
$R_p = 17.6$, $R_{wp} = 19.0$, $R_e = 7.5$, $\chi^2 = 6.4$						

Table 2
Structural parameters for the binary compound Nd_5Ni_{19} showing coexistence of two isotypic forms of Nd_5Ni_{19}: 2*H* (space group *P*6$_3$/*mmc*) and 3*R* (space group *R*-3*m*). A third minor phase is detected: $NdNi_5$ with $CaCu_5$ type structure.

Phases	Atoms	Sites	*x*	*y*	*z*	Occ.
Nd_5Ni_{19} Pr_5Co_{19}-type	Pr	$2c_1$	1/3	2/3	1/4	1
	Pr	$4f_1$	1/3	2/3	0.133(2)	1
	Pr	$4f_2$	1/3	2/3	0.020(2)	1
	Ni	$2a_1$	0	0	0	1
	Ni	$2b_1$	0	0	1/4	1
	Ni	$2d_1$	1/3	2/3	3/4	1
	Ni	$4e_1$	0	0	0.125	1
	Ni	$4f_3$	1/3	2/3	0.875(5)	1
	Ni	$12k_1$	0.842(9)	2x	0.065(3)	1
	Ni	$12k_2$	0.822(9)	2x	0.186(1)	1
Phase 2*H*-*P*6$_3$/*mmc*; 42 wt%; $a = 4.987(1)$ Å; $c = 32.35(2)$ Å; *V*/unit cell = 696.5(4) Å^3; $R_{bragg} = 11.7$; $R_f = 8.7$						
Nd_5Ni_{19} Ce_5Co_{19}-type	Pr	$3a_1$	0	0	0	1
	Pr	$6c_1$	0	0	0.0791(8)	1
	Pr	$6c_2$	0	0	0.1519(7)	1
	Ni	$3b_1$	0	0	1/2	1
	Ni	$6c_3$	0	0	1/4	1
	Ni	$6c_4$	0	0	1/3	1
	Ni	$6c_5$	0	0	0.413(2)	1
	Ni	$18h_1$	1/2	1/2	0.122(1)	1
	Ni	$18h_2$	1/2	1/2	0.0410(1)	1
Phase 3*R*-*R*-3*m*; 53 wt%; $a = 4.990(1)$ Å; $c = 48.57(1)$ Å; *V*/unit cell = 1047.7(4) Å^3; $R_{bragg} = 9.7$; $R_f = 7.19$						
$NdNi_5$ $CaCu_5$-type	Pr	1*a*	0	0	0	1
	Ni	2*c*	1/3	2/3	0	1
	Ni	3*g*	1/2	0	1/2	1
Phase 2*H*-*P*6/*mmm*; 5 wt%; $a = 4.964(6)$ Å; $c = 3.961(4)$ Å; *V*/unit cell = 84.5(2) Å^3; $R_{bragg} = 11.4$; $R_f = 6.6$						
$R_p = 21.9$, $R_{wp} = 24.8$, $R_e = 8.2$, $\chi^2 = 9.3$						

gives a global composition of the compounds. The results are $PrNi_{(3.94\pm0.07)}$ and $NdNi_{(3.96\pm0.13)}$. Both are superior to the expected stoichiometry and the EPMA results. Those differences can be explained by taking into account 7 wt% and 5 wt% of respectively $PrNi_5$ and $NdNi_5$ in the global composition.

3.2. Gas hydrogenation properties

Both compounds easily absorb hydrogen at room temperature. For the binary Pr_5Ni_{19}, the maximum capacity reaches 1.33 wt% at room temperature (25 °C) and under 10 MPa of hydrogen and is obtained for the first cycle. For Nd_5Ni_{19}, the maximum capacity is 1.17 wt% under the same experimental conditions.

The capacity of both compounds decreases for each following cycles, indicating some irreversible process during cycling. The plateau pressure and capacity are summarized in Table 3. The absorption and desorption curves measured at 25 °C and 40 °C for Pr_5Ni_{19} and Nd_5Ni_{19} are shown respectively in Fig. 3(a) and (b). For both compounds, we observe no differences between 2*H* and 3*R* phases and a plateau for absorption and desorption. Each PCT curve can be decomposed in three different parts. First, an increasing branch at low capacity typical of the α-phase is observed, then a plateau corresponding to a two-phase domain (α to β transformation) appears, and finally a second increasing branch corresponding to the β-phase.

Table 3
Capacity and pressure plateau of Pr_5Ni_{19} and Nd_5Ni_{19} at 25 and 40 °C.

	Cycle condition	Capacity (wt%)	Desorption plateau pressure (MPa)
Pr_5Ni_{19}	Cycle 1, 25 °C	1.33(6)	–
	Cycle 3, 25 °C	1.05(6)	0.80(4)
	Cycle 4, 40 °C	0.95(6)	1.05(5)
Nd_5Ni_{19}	Cycle 1, 25 °C	1.17(6)	–
	Cycle 4, 25 °C	0.98(6)	1.0(5)
	Cycle 5, 40 °C	0.84(6)	1.9(1)

From a careful examination of the PCT curves, the occurrence of another plateau for capacity larger than 0.7 wt% cannot be totally ruled out. However, additional measurements at lower temperature or in situ neutron powder diffraction would be necessary to ensure the existence or not of such plateau at high pressure.

4. Discussion

Pr_5Ni_{19} and Nd_5Ni_{19} are not mentioned in phase-diagrams of Pr–Ni and Nd–Ni binary systems [10,11]. This study shows that both phases exist and they can be obtained after long annealing time, 35 days, at 1100 °C.

La_5Ni_{19} is stable at high temperature but will decompose into La_2Ni_7 and $LaNi_5$ at lower temperature [2]. Assuming that Nd_5Ni_{19} and Pr_5Ni_{19} phases exhibit the same behaviour and a very narrow domain of existence, it would be very difficult to avoid the formation of some $PrNi_5$ or $NdNi_5$ phase in the obtained compounds.

Like the La_5Ni_{19} compound [13], two types of structures are known for those phases: the 2*H* hexagonal one and the 3*R* rhombohedral one. In the present work, both structures are observed. The 2*H* one is the low temperature phase and the 3*R* one is the high temperature phase. It seems that the rhombohedral–hexagonal transformation is a non diffusion process. As soon as the rhombohedral phase is formed it is not possible to turn it into the hexagonal phase by annealing, no matter the temperature or the duration of the annealing [14].

Considering their quite similar structures, 2*H* and 3*R* are expected to have close behaviour regarding hydrogenation properties. In the two systems, the PCT curves show only one plateau without any step allowing to distinguish the sorption properties of 2*H* or 3*R*. This is not surprising when the volume of the stacking unit $[A_2B_4]/3[AB_5]$ is taken into consideration. Plateau pressure is related to the volume of the stacking unit. This volume can be obtained from the unit cell volume $V = \sqrt{3}a^2 \times c/2$ as $V/2$ for the 2*H* phase and $V/3$ for the 3*R* one. That leads to very close volume of the stacking units for both 2*H* and 3*R* in Nd_5Ni_{19} and Pr_5Ni_{19} cases.

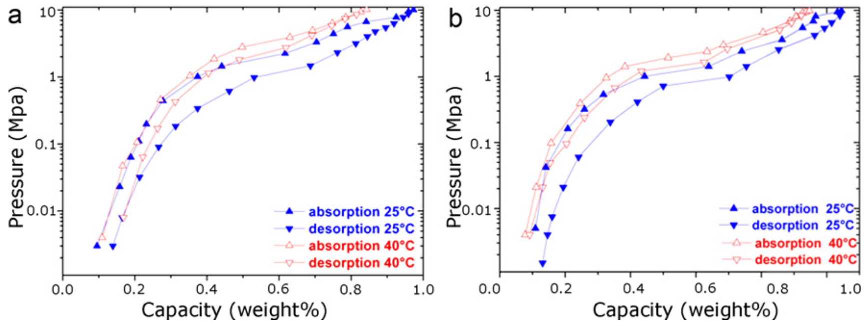

Fig. 3. PCT curves for Pr_5Ni_{19} (a) and Nd_5Ni_{19} (b) compound measured at 25 °C and 40 °C up to 10 MPa of hydrogen showing one plateau in absorption and desorption.

With those close volumes, no differences in plateau pressure are expected for 2*H* and 3*R*. The two hydrides have their plateau close to 1 MPa, a higher value than for La_5Ni_{19} [13]. This can be explained by the smaller atomic radius of Pr and Nd compared to La. Losses of capacities are observed for the two compounds upon cycling. This phenomenon has already been observed for La_5Ni_{19}. The crystallographic structure of the A_5B_{19} phases can be decomposed as A_2B_4 and AB_5 subunits [15].

While AB_5 compounds are stable upon cycling [16], A_2B_4 compounds are known to undergo a partial amorphization when hydrogenated [17]. During successive hydrogenations, the A_2B_4 units are subjected to progressive amorphization responsible for the capacity decrease.

5. Conclusion

The compounds Pr_5Ni_{19} and Nd_5Ni_{19} have been synthesized and investigated regarding structural and thermodynamic properties. Both 2*H* and 3*R* structures coexist for both binary compounds. Those compounds absorb hydrogen easily at room temperature in the range of 0–10 MPa. No differences regarding hydrogen properties are found between 2*H* and 3*R*. The plateau pressures need to be lowered if one wants to use them as battery materials.

Mg substitution on the Pr or Nd sublattice and other substitutions on the Ni sublattice are planned to decrease the working pressure and to improve the cycle life.

Acknowledgements

The authors are thankful to Mr E. Leroy for technical assistance in the EPMA analysis and to Mrs D. Dragoe for technical assistance in the ICP-OES analysis.

References

[1] T. Kohno, H. Yoshida, F. Kawashima, T. Inaba, I. Sakai, M. Yamamoto, M. Kanda, Journal of Alloys and Compounds 311 (2000) L5–L7.

[2] T. Yamamoto, H. Inui, M. Yamaguchi, K. Sato, S. Fujitani, I. Yonezu, K. Nishio, Acta Materialia 45 (1997) 5213–5221.

[3] H. Inui, T. Yamamoto, Z. Di, M. Yamaguchi, Journal of Alloys and Compounds 293–295 (1999) 140–145.

[4] Z. Di, T. Yamamoto, H. Inui, M. Yamaguchi, Intermetallics 8 (2000) 391–397.

[5] T. Ozaki, M. Kanemoto, T. Kakeya, Y. Kitano, M. Kuzuhara, M. Watada, S. Tanase, T. Sakai, Journal of Alloys and Compounds, Proceedings of the International Symposium on Metal–Hydrogen Systems, Fundamentals and Applications (MH2006) 446–447 (2007) 620–624.

[6] A. Ferey, Elaboration and characterization of ABx (A = La, Mg B = Ni and *x* = 3–4) hydride forming alloys to be used as active materials for negative electrode of NiMH battery, Thesis, University of Paris Est Créteil, 2008. http://www.dart-europe.eu/full.php?id=180503.

[7] H.E. Hayakawa, H.E. Akiba, Journal of the Japan Institute of Metals 70 (2006) 158–161.

[8] J.I. Nakamura, K. Hayakawa, H. Nakamura, Y.E. Akiba, Journal of Physical Chemistry C 113 (2009) 5853–5859.

[9] Q.F. Zhang, M. Si, T. Fanf, F.D. Sun, Journal of Physical Chemistry C 114 (2010) 11686–11692.

[10] H. Okamoto, Journal of Phase Equilibria and Diffusion 26 (2005) 650.

[11] H. Okamoto, Journal of Phase Equilibria and Diffusion 27 (2006) 552.

[12] J. Rodríguez-Carvajal, Fullprof: a program for Rietveld refinement and pattern matching analysis, Physica B 192 (1993) 55–69.

[13] A. Férey, F. Cuevas, M. Latroche, B. Knosp, P. Bernard, Electrochimica Acta 54 (2009) 1710–1714.

[14] K.H.J. Buschow, A.S. Van Der Goot, Journal of the Less Common Metals 22 (1970) 419–428.

[15] E. Akiba, H. Hayakawa, T. Kohno, Journal of Alloys and Compounds, Proceedings of Rare Earths'04 in Nara, Japan, Proceedings of Rare Earths'04 408–412 (2006) 280–283.

[16] H. Oesterreicher, J. Clinton, H. Bittner, Materials Research Bulletin 11 (1976) 1241–1247.

[17] V. Paul-Boncour, C. Lartigue, A. Percheron-Guégan, J.C. Achard, J. Pannetier, Journal of the Less Common Metals 143 (1988) 301–313.